Polymer Chemistry

Cite this: DOI: 10.1039/c2py00533f

www.rsc.org/polymers

PAPER

Development of thermosensitive copolymers of poly(2-methoxyethyl acrylate-*co*-poly(ethylene glycol) methyl ether acrylate) and their nanogels synthesized by RAFT dispersion polymerization in water†

Guangyao Liu, Qian Qiu and Zesheng An*

Received 9th November 2011, Accepted 7th December 2011
DOI: 10.1039/c2py00533f

Thermosensitive polymeric materials based on copolymers of oligo(ethylene glycol) methacrylates are attracting significant attention in various materials sectors. The preparation of their thermosensitive microgels/nanogels *via* the aqueous dispersion polymerization process is, however, limited by low monomer loading and thus low solid content of the final colloids. Moreover, the preparation of nanogels by reversible addition-fragmentation chain transfer (RAFT) mediated dispersion polymerization has been further hampered by the poor RAFT control of the polymerization process. In this article, we report the development of thermosensitive copolymers based on poly(2-methoxyethyl acrylate-*co*-poly(ethylene glycol) methyl ether acrylate) (P(MEA-*co*-PEGA)) and their use for nanogel synthesis by RAFT dispersion polymerization in water. The thermosensitive copolymers exhibited sharp thermal transitions upon increasing thee temperature above their lower critical solution temperature. The use of MEA as the majority comonomer and poly(*N*,*N*′-dimethylacrylamide) as the RAFT agent and stabilizer for the synthesis of nanogels allowed monomer loadings of up to 20%, which significantly improved the solid content of the dispersion polymerization system. Moreover, the dispersion copolymerization of MEA with PEGA was under excellent RAFT control up to complete monomer conversion. The synthesized nanogels showed an unprecedented linear relationship between nanogel size and temperature, suggesting expanded applications of such responsive polymeric materials.

Introduction

Smart or responsive polymeric materials[1,2] have been playing an important role in the development of advanced technologies including actuators and sensors,[3–5] shape memory devices,[6,7] switchable surfaces,[8–10] tissue engineering scaffolds,[11,12] drug/protein/gene delivery vectors,[13–15] reaction vessels and catalysts,[16] and optical and electronic devices.[17–19] Among them, thermosensitive polymers[20,21] are a common class of responsive materials that change their solution properties in response to the variation in temperature, which is a convenient stimulus to apply externally. Indeed, various types of thermosensitive polymers have been developed thus far with the most prominent example being poly(*N*-isopropylacrylamide) (PNIPAM), which has a lower critical solution temperature (LCST) around 32 °C.[21] PNIPAMs have been widely used in biologically relevant areas because their LCST is around body temperature and is relatively insensitive to the variation in molecular weight and electrolyte concentration. However, several drawbacks of PNIPAMs have limited their further applications, which include hysteresis upon cooling from above the LCST, possible hydrogen-bonding interaction with proteins and toxicity of its monomer. Therefore, significant current research is devoted to the pursuit of PNIPAM alternatives that can maintain their favourable properties but minimize their drawbacks.[22–24] One of such emerging materials is copolymers based on oligo(ethylene glycol) methacrylates (OEGMAs),[25–27] and recent years have witnessed increasing study and their application in diverse materials arenas.[28–44] The current intensive interest in OEGMA copolymers originates from several attractive features such as biocompatibility, complete reversibility of thermal transition, adjustable LCST, and antifouling properties at temperatures lower than the LCST.[45–47]

The thermosensitivity of polymers can be exploited for the preparation of responsive microgels and nanogels.[48] As thermosensitive OEGMA copolymers are gaining popularity in materials science, their use in the preparation of microgels and nanogels has also been studied.[49] Hu and co-workers[50] reported the first preparation of microgels by free-radical precipitation polymerization in water of 2-(2-methoxyethoxy)ethyl methacrylate (MEO_2MA) and OEGMA ($OEGMA_{475}$ or $OEGMA_{300}$, for

Institute of Nanochemistry and Nanobiology, College of Environmental and Chemical Engineering, Shanghai University, Shanghai, P. R. China 200444. E-mail: an.zesheng@shu.edu.cn; Fax: +86-21-66135275; Tel: +86-21-66135277

† Electronic supplementary information (ESI) available. See DOI: 10.1039/c2py00533f

M_n = 475 or 300), which they subsequently assembled into photonic hydrogels.[51] Later, the same group reported the preparation of core-shell microgels based on OEGMAs *via* seeded precipitation polymerization.[52] Recently, Zhou and co-workers studied the possibility of drug release from such microgels.[53] The preparation of microgels of OEGMAs using controlled radical polymerization techniques has also been reported. In miniemulsion using anisole as the organic phase and *via* activators generated by electron transfer for atom transfer radical polymerization (AGET ATRP), Matyjaszewski and co-workers reported the preparation of microgels of MEO_2MA loaded with magnetic nanoparticles and microgels of tunable LCST based on copolymers of MEO_2MA and OEGMA.[54,55] On extending reversible addition-fragmentation chain transfer (RAFT) mediated aqueous precipitation/dispersion polymerization for the synthesis core-shell nanogels,[56,57] our group has reported the preparation of core-shell nanogels based on copolymers of MEO_2MA and $OEGMA_{475}$.[58] The shell polymers consisted of either linear poly(ethylene glycol) (PEG) or graft poly-$OEGMA_{475}$, and the core polymers consisted of copolymers of MEO_2MA and $OEGMA_{475}$ of varied molar ratios, which were cross-linked by poly(ethylene glycol) dimethacrylate (M_n = 750). The nanogels with graft poly$OEGMA_{475}$ as the shell polymer exhibited enhanced stability during freeze-thawing process and in biologically relevant solutions such as 1.5 M NaCl, 1% bovine serum albumin and 100% fetal bovine serum. Also the nanogels exhibited excellent biocompatibility through cell viability studies.

Even with the aforementioned success in the preparation of microgels and nanogels based on polymers of MEO_2MA or copolymers of MEO_2MA with OEGMA, several limitations associated with each synthetic method can be identified. In the microgel synthesis by AGET ATRP miniemulsion, an organic phase had to be used.[54,55] Although the (co)polymers MEO_2MA and OEGMA exhibited sharp LCST transitions in water, the phase transitions of the corresponding microgels were broader.[54] Provided that the molecular weights of the copolymers synthesized in AGET ATRP miniemulsion were well controlled with low polydispersities, the broadening in the phase transitions of the corresponding microgels may be due to the restriction in the polymer freedom and the crowding of such graft polymers in the networks. In the microgel synthesis by free-radical precipitation polymerization, although the microgels were highly monodisperse, the solids content was only $\leq$ 2% w/v.[50] This situation also applies to the core-shell nanogels synthesized by RAFT mediated dispersion polymerization in which the monomer loading was restricted to ~2% w/v, although a total solid content of up to 5% w/v could be achieved with the macromolecular chain transfer agent (Macro-CTA) included.[58] This low solid content is exerted by the poor solubility of MEO_2MA in water. In the latter two cases,[50,58] the phase transitions were significantly broad, even broader than that for microgels synthesized in a miniemulsion by AGET ATRP.[54] For the microgels synthesized by free-radical precipitation polymerization,[50,52] the broad phase transition was attributed to the broad distribution of molecular weight as expected for polymers synthesized by traditional free-radical polymerization. The broadening in the phase transition for the nanogels synthesized by RAFT-mediated dispersion polymerization was, however, unexpected, which might be attributed to both the relatively poor control of the molecular weight distribution and the network restriction of the graft type polymers.[58] The relatively poor RAFT control in the dispersion polymerization of MEO_2MA and OEGMA may be ascribed to 1) the methacrylate type of the monomers, which can be difficult to control by the RAFT dispersion polymerization process, and 2) the steric effect of both the monomers with various side chain lengths and the graft shell polymer, which restricts the entry of the monomers or monomeric/oligomeric radical species into the nanogels.

In order to solve these problems, it is crucial to develop new thermosensitive copolymers that are structurally similar to the MEO_2MA and OEGMA copolymers such that the associated desirable properties can be retained but their nanogels can be synthesized at higher solid content and their dispersion polymerization can be controlled by the RAFT process. We have recently found that 2-methoxyethyl acrylate (MEA) is highly soluble in water but its polymer PMEA is not.[59] Successful RAFT-mediated aqueous dispersion polymerization has been established with monomer loading up to 25% w/v and solid content up to 32% w/v, in which the polymerization process was under excellent RAFT control and polymers with low polydispersity indices were produced.[59] Although PMEA is not water soluble, it should still possess a certain degree of polarity since MEA is highly soluble in water and very polar. Indeed, PMEA has been used as a hemocompatible material due to the formation of a layer of freezing bound water to the polymer surface.[60,61] It is known that by adjusting the subtle balance between the hydrophilicity and hydrophobicity of polymers through copolymerization of judiciously selected comonomers, thermosensitive copolymers of adjustable LCST can be produced depending on the constitution and composition of the copolymers. We therefore anticipate that copolymerization of MEA with oligo (ethylene glycol) methyl ether acrylate (OEGA) should produce a set of thermosensitive copolymers that are similar in structure and properties to the MEO_2MA and OEGMA copolymers. Of particularly important is that the use of MEA as the majority comonomer is expected to produce nanogels at high solid content because of its high water solubility. Furthermore, MEA has a smaller side chain than MEO_2MA and is therefore expected to have a smaller steric hindrance to enter the nanogels for RAFT dispersion polymerization. Previously, thermosensitive copolymers of 2-(2-ethoxyethoxy)ethyl acrylate and OEGA (M_n = 454) were reported.[62] However, our own experience indicated that 2-(2-ethoxyethoxy)ethyl acrylate has an even lower water solubility than MEO_2MA and thus is not suitable for the preparation of nanogels at high solids content. Steinhauer and co-workers[63] reported the copolymerization of MEA with 2-hydroxyethyl acrylate *via* RAFT to produce thermosensitive copolymers but their use in the preparation of nanogels was not demonstrated. Very recently, Lavigueur and co-workers prepared thermosensitive copolymers of MEA with methoxy ethoxy ethyl acrylate using ATRP, which were then conjugated to green fluorescent protein to make thermosensitive giant biohybrid amphiphiles.[64] Because methoxy ethoxy ethyl acrylate is only one ethylene glycol unit longer than MEA, the LCST range of their copolymers should be narrower than that would be expected for copolymers of MEA and OEGA with longer side chains. Therefore, we decided to investigate the thermosensitivity of copolymers of MEA and OEGA and their use in the synthesis of

nanogels *via* RAFT-mediated aqueous dispersion polymerization aiming at developing a new platform for thermosensitive polymeric materials.

Results and discussion

Synthesis and characterization of thermosensitive copolymers

A series of thermosentitive copolymers of MEA with poly (ethylene glycol) methyl ether acrylate (PEGA, $M_n = 480$) was synthesized by RAFT using benzyl ethyl trithiocarbonate as the chain transfer agent (CTA) and AIBN as the initiator at 70 °C in DMF (Scheme 1). The molar ratio of MEA and PEGA was varied from 9 : 1 to 7 : 3 to adjust the LCST of the copolymers. In order to gain more information on the copolymerization kinetics, homopolymerization of MEA and PEGA was also performed. For all homopolymers and copolymers, the target degree of polymerization (DP) was ~100 and the conversion of monomers was above 90% (Table 1). The composition of the polymers was characterized by ^{1}H NMR (Fig. S1†) and the macromolecular characteristics were characterized by gel permeation chromatography (GPC).

Fig. 1 shows the polymerization kinetics of homopolymerization of MEA and PEGA and copolymerization of MEA with PEGA at molar ratios of 90 : 10 and 70 : 30. In all cases, the monomer conversion increases very rapidly within 1 h and the polymerization essentially levels off after 2 h.

The homopolymerization of MEA is faster than that of PEGA. The polymerization of MEA is under excellent RAFT control as evidenced by the symmetric and monomodal GPC chromatograms up to high monomer conversion (94%), low polydispersity index (1.15) and the linear increment of M_n with conversion (Fig. 2 and 3). The homopolymerization of PEGA is also under good RAFT control with monomer conversion up to 60% since its GPC chromatogram at this point is symmetric and the polydispersity index is low (1.22). However, its GPC chromatograms become increasingly unsymmetric above 60% monomer conversion and the polydispersity index correspondingly increases to 1.46 at 92% conversion, although a reasonably good linearity between M_n and monomer conversion is still observed over the entire range of monomer conversion (Fig. 2 and 3). Because PEGA monomer has a relatively long side chain and the polymer is a comb or graft conformation, as the polymerization continues and the molecular weight increases, the steric congestion at the polymer end becomes increasingly significant, preventing further addition of monomers, resulting in the off-optimal behaviour of the RAFT process. The higher-molecular-weight shoulders for PEGA homopolymers above 60% monomer conversion may possibly come from two sources. One is bimolecular termination and the other is transfer to chain. Given the high steric congestion at the polymer end at high monomer conversion, the former is less likely to occur. One of the major side reactions in controlled radical polymerization of acrylate is transfer to chain,[65–67] which leads to the formation of branched polymers with higher molecular weight. It should be noted that for similar absolute molecular weight, branched structure has smaller molecular weight (more compact structure). However, transfer to chain reaction may add more than one polymer chains to an existing one, and therefore chain transfer leads to higher molecular weight. Transfer to solvent (DMF) is less likely to occur since transfer to solvent should lead to a lower molecular weight. Analysis of $\ln(M_0/M)$ *vs.* time indicated reduced polymerization rate at high monomer conversion possibly due to radical transfer reactions (Fig S3†). Since both further addition of monomer and bimolecular termination become difficult at high monomer conversion, the possibility of transfer to chain becomes significant and should be the main reason for the broadening in the GPC chromatograms of PPEGA.

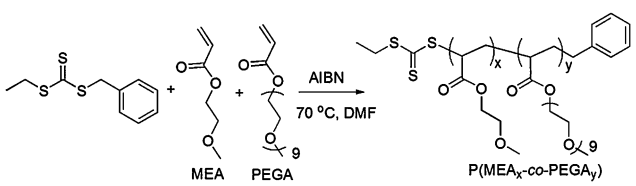

Scheme 1 Synthesis of thermosenstitive copolymers of MEA with PEGA

For the copolymerizations, MEA was used as the majority monomer and PEGA content was increased up to 30 mol%. Although homopolymerization of PEGA is slower than that of MEA, the copolymerization rate of MEA with PEGA is, however, the same regardless of the molar ratio difference (Fig. 1). This can be explained on the basis of the low content of PEGA in the copolymers; the random copolymerization of low molar fraction of PEGA with MEA alleviates the steric constraint that is present in PEGA homopolymer and thus PEGA can be incorporated at essentially the same rate as MEA. If this is true, it is expected that increasing PEGA molar fraction will gradually increase the steric hindrance for incorporation of PEGA into the copolymers, which will consequently become gradually less well-controlled by the RAFT process. Indeed, examination of the GPC chromatograms of the copolymers at high monomer conversions indicates that the higher-molecular-weight shoulder for P(MEA$_{70}$-*co*-PEGA$_{30}$) is slightly more prominent than that for P(MEA$_{86}$-*co*-PEGA$_{10}$), and copolymers with increasing PEGA molar fraction also show higher polydispersity index (Table 1). In addition, all the copolymers produced have low polydispersity indices (≤1.25) at high monomer conversions (92–97%) and a fairly good linear relationship between M_n and monomer conversion (Fig. 2).

With the set of well-defined copolymers of similar DP being successfully synthesized, their thermal transitions were characterized in water at a concentration of 1 wt% (Fig. 4). All the copolymers display sharp response to temperature change upon heating through their LCST. The LCST of the copolymers increases with increasing molar fraction of the more hydrophilic monomer PEGA, as expected. A linear relationship is observed between the LCST and PEGA molar fraction. From the fitted line, it can be easily calculated that 14% PEGA incorporation will bring the LCST of the copolymer to the body temperature (37 °C). A convenient temperature range (from room temperature to 65 °C) can be realized by incorporation of less than 30 mol% PEGA, at which point the synthesis of the copolymer is still under good RAFT control. Therefore, this set of thermosensitive copolymers based on MEA and PEGA should nicely complement the copolymers based on MEO_2MA and OEGMA

Table 1 Synthetic conditions and results of homopolymers and thermosensitive copolymers.[a]

	MEA	PEGA	Time (h)	Conv. (%)[b]	M_n (theoretical)[c]	M_n (GPC)[d]	M_w/M_n (GPC)[d]	LCST (°C)[e]
$PMEA_{97}$	103	0	3	94	13 000	24 000	1.15	
$P(MEA_{86}$-*co*-$PEGA_{10})$	93	10	3	92	15 000	30 000	1.15	29
$P(MEA_{84}$-*co*-$PEGA_{15})$	88	16	6	95	18 000	26 000	1.23	40
$P(MEA_{76}$-*co*-$PEGA_{18})$	83	20	5	92	19 000	33 000	1.19	48
$P(MEA_{75}$-*co*-$PEGA_{25})$	78	26	6	97	21 000	29 000	1.24	57
$P(MEA_{70}$-*co*-$PEGA_{30})$	72	32	3	97	23 000	31 000	1.25	64
$PPEGA_{97}$	0	105	3.5	92	44 000	41 000	1.46	

[a] Target DP = ~100 (the target MEA and PEGA are listed as molar ratios), [CTA] = 29 mM, AIBN : CTA = 0.2 : 1, 70 °C. [b] Monomer conversion determined by ^{1}H NMR. [c] Theoretical molecular weight of homopolymers = (target DP × monomer conversion) × $M_{monomer}$ + M_{CTA}; theoretical molecular weight of copolymers = (target DP_{MEA} × monomer conversion) × M_{MEA} + (target DP_{PEGA} × monomer conversion) × M_{PEGA} + M_{CTA}. [d] Molecular weight determined by GPC (DMF, PMMA). [e] The temperature at 50% transmittance of the thermal transition was taken as the LCST.

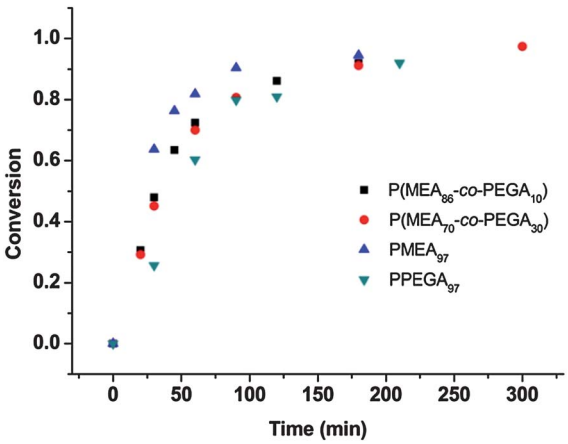

Fig. 1 Polymerization kinetics of homopolymerization of MEA and PEGA and their copolymerization. [CTA] = 29 mM in DMF, [CTA] : [AIBN] : [monomer] = 1 : 0.2 : 100, 70 °C.

developed by Lutz and Hoth.[25] More importantly and particularly relevant to the following work is the high water solubility of MEA, in contrast to the poor solubility of MEO_2MA, which makes MEA ideal for the preparation of thermosensitive nanogels by aqueous dispersion copolymerization with PEGA.

RAFT dispersion polymerization for the synthesis of nanogels

Nanogel synthesis by RAFT-mediated heterogeneous polymerization allows facile control of molecular weight/polydispersity, the localization of functionality and a significant degree of architectural design.[48] For example, Lu and co-workers developed a novel methodology for the production of hollow nanogels (nanocapsules) by the combination of RAFT with inverse miniemulsion.[68] Later, Wang and co-workers nicely extended Lu's approach to synthesize cross-linked hollow nanogels.[69] In both cases, polymers with low polydispersity were produced, characteristic of the RAFT control.[68,69] We[56–58] and others[70–72] have been working on RAFT-mediated dispersion polymerization in water for the synthesis of nanogels. We have also recently demonstrated the efficient and versatile synthesis of core-cross-linked star polymers with low polydispersity in RAFT-mediated dispersion and emulsion polymerizations.[73] This strategy combines polymerization and self assembly of the *in situ* produced responsive block copolymers in one pot and produces

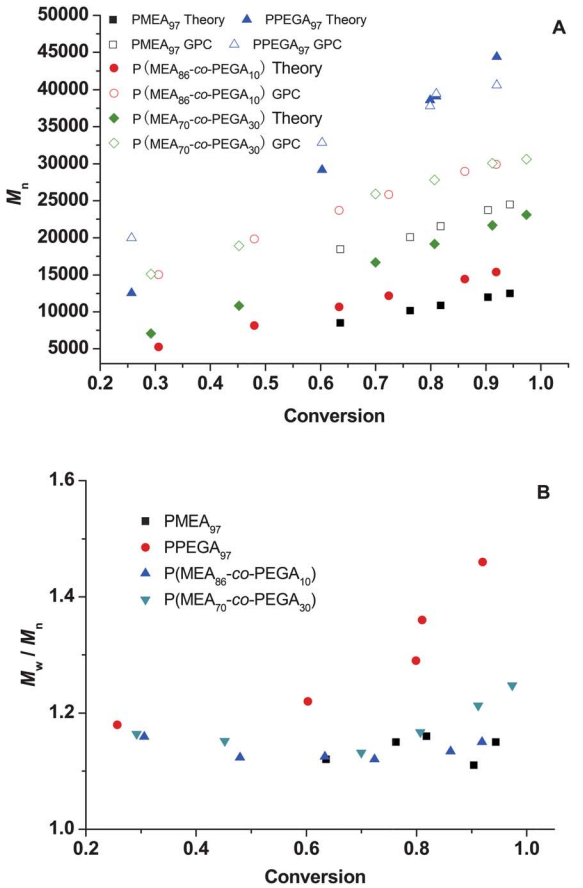

Fig. 2 Molecular weight (A) and polydispersity index (B) revolution with monomer conversion of MEA and PEGA homopolymers and their copolymers. [CTA] = 29 mM in DMF, [CTA] : [AIBN] : [monomer] = 1 : 0.2 : 100, 70 °C.

defined nanogels or star polymers. Through the macro-CTA design, the corresponding functional groups can be transferred to the nanogel's core and/or shell, providing convenient handles for installing active agents for biomedical applications.[57]

With the development of well-defined thermosensitive copolymers of MEA with PEGA, we further examined their use for the preparation of thermosensitive nanogels by RAFT dispersion polymerization in water. The use of MEA as the majority comonomer is expected to significantly improve the solid content since MEA is highly soluble in water, which is in stark contrast to

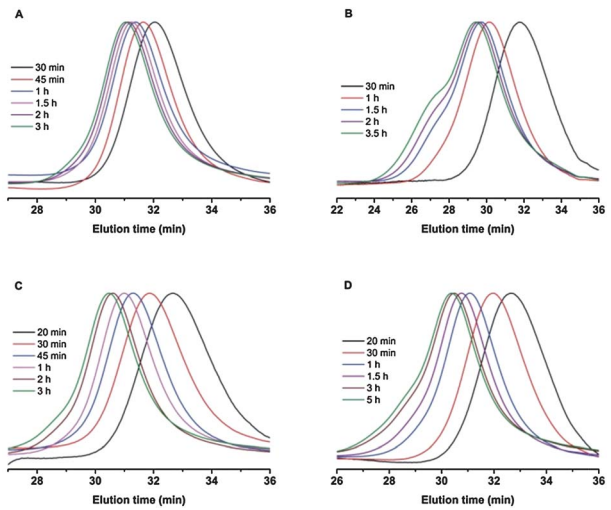

Fig. 3 GPC chromatograms at different polymerization times for the synthesis of $PMEA_{97}$ (A), $PPEGA_{97}$ (B), $P(MEA_{86}$-*co*-$PEGA_{10})$ (C), and $P(MEA_{70}$-*co*-$PEGA_{30})$ (D). [CTA] = 29 mM in DMF, [CTA] : [AIBN] : [monomer] = 1 : 0.2 : 100, 70 °C.

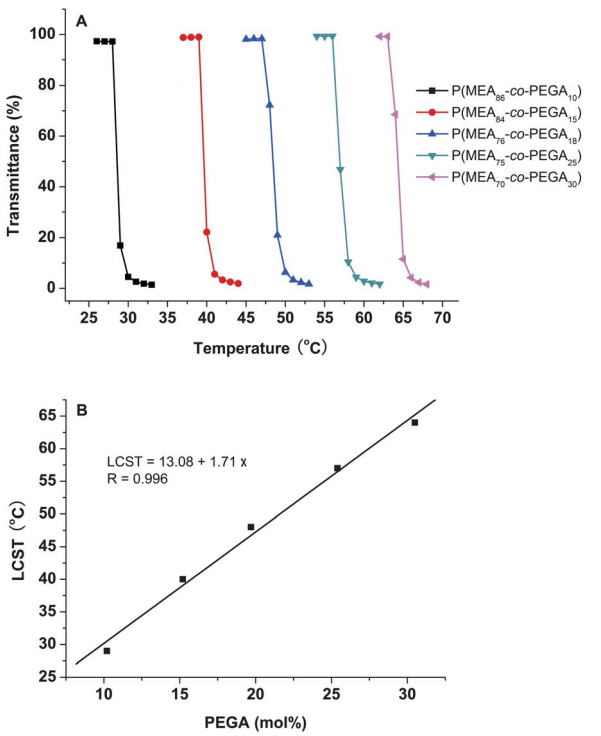

Fig. 4 Thermal transitions of the copolymers measured by turbidimetry with 1 wt% polymer in water (A) and dependence of LCST of the copolymers on PEGA molar fraction (B).

the nanogel synthesis using MEO_2MA as the majority comonomer.[58] Since the RAFT dispersion copolymerization of MEO_2MA with OEGMA showed relatively poor RAFT control, it is also interesting to see whether dispersion copolymerization of MEA with PEGA could be controlled by the RAFT process.

In the RAFT dispersion copolymerization (Scheme 2), poly(*N*,*N*′-dimethylacrylamide) (PDMA) was used as the Macro-CTA, which was synthesized at 61% monomer conversion to ensure a high degree of CTA end function. The theoretical M_n of PDMA was 5 k as calculated from the monomer conversion determined by ^{1}H NMR, and the GPC M_n was 8 k and M_w/M_n was 1.10. PDMA was previously demonstrated to be an efficient Macro-CTA in the RAFT control of acrylics in emulsion polymerization of butyl acrylate,[74] and dispersion polymerization of *N*-isopropylacrylamide[56,57] and *N*,*N*′-diethylacrylamide.[70,72] Therefore, the synthesized PDMA with low polydispersity is well positioned for the RAFT dispersion copolymerization of MEA with PEGA. Significantly, the total monomer content was controlled ≥10% w/v, which is much higher than the ~2% w/v monomer content in the case of dispersion copolymerization of MEO_2MA with OEGMA. In nanogel synthesis poly(ethylene glycol) diacrylate (PEGDA, M_n = 258) was used as the cross-linker and 2,2′-azobis(2-methylpropionamidine) dihydrochioride (V-50) was used as the initiator. The molar ratio of PDMA: PEGDA was controlled at a constant value of 1 : 3. The molar ratio of PDMA:V-50 was controlled at 1 : 0.05, which was designed to minimize side reactions such as transfer to chain in the polymerization of acrylate.[66,67]

The dispersion copolymerization kinetics without PEGDA cross-linker is illustrated in Fig. 5A for two copolymerization systems with the molar ratio of MEA : PEGA being 90 : 10 and 85 : 15, respectively. As can be seen, the polymerization rate is fairly fast with over 90% monomer conversion being achieved within 2 h, considering that a low concentration of V-50 was used. The polymerization kinetics are essentially the same for the two systems regardless of the different comonomer molar ratios, which is consistent with the results of homogeneous copolymerization in DMF. As shown in Fig. 5B, the M_n of the produced block copolymer PDMA-*b*-P(MEA-*co*-PEGA) evolves linearly with increasing monomer conversion up to almost complete monomer consumption, and the polydispersity index (M_w/M_n) of the block copolymer remains below 1.15. GPC chromatograms (Fig. 6) show a clear shift to higher molecular weight side with increasing polymerization time and thus increasing monomer conversion. The PDMA macro-CTA is highly efficient for the RAFT dispersion copolymerization of MEA with PEGA, which is almost completely consumed with 30 min, thus suggesting excellent blocking efficiency under dispersion polymerization conditions. Although the M_w/M_n of all the produced block copolymers is lower than 1.15, there is an obvious shoulder at the higher-molecular-weight side of all the chromatograms regardless of monomer conversion, and the shoulder is increasingly pronounced with increasing monomer conversion. This can be mainly attributed to transfer to chain,

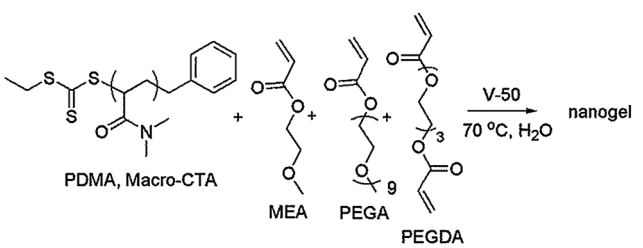

Scheme 2 Synthesis of thermosensitive nanogels of MEA and PEGA using PDMA macro-CTA in water.

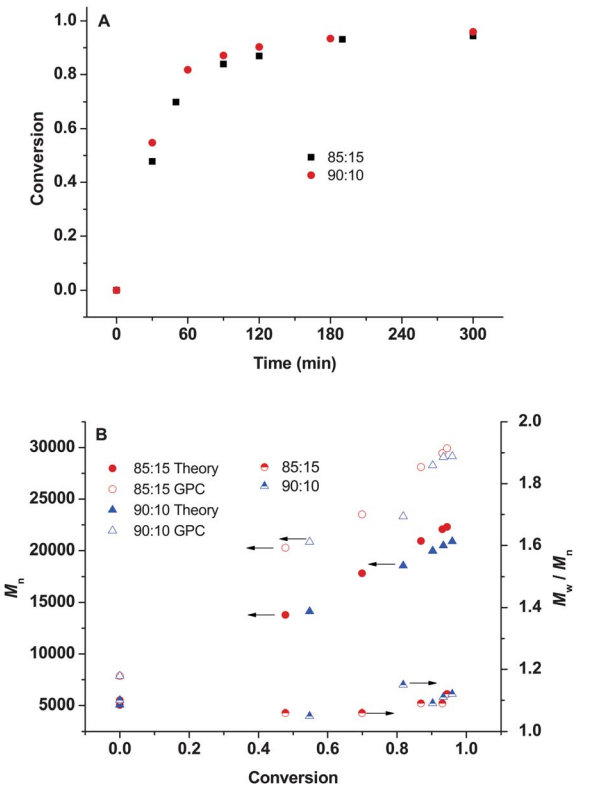

Fig. 5 (A) Polymerization kinetics and (B) evolution of molecular weights and polydispersity indices of PDMA-*b*-P(MEA-*co*-PEGA), synthesized by dispersion copolymerization of MEA with PEGA using PDMA Macro-CTA in water. Monomer content = 10% (w/v), [macro-CTA] : [MEA + PEGA] : [V-50] = 1 : 100 : 0.05, 70 °C.

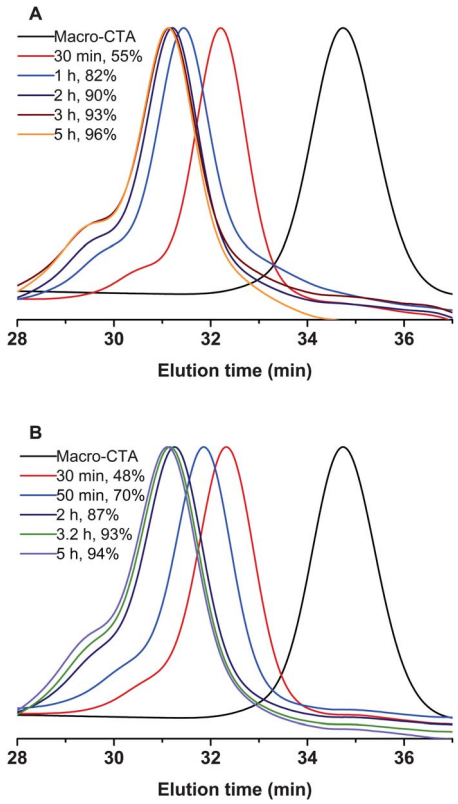

Fig. 6 GPC chromatograms of (A) PDMA-*b*-P(MEA_{90}-*co*-$PEGA_{10}$) and (B) PDMA-*b*-P(MEA_{85}-*co*-$PEGA_{15}$) polymers at different monomer conversions, synthesized by dispersion copolymerization of MEA with PEGA using PDMA macro-CTA in water. Monomer content = 10% (w/v), [macro-CTA] : [MEA + PEGA] : [V-50] = 1 : 100 : 0.05, 70 °C.

which is related to reaction conditions such as temperature and radical concentration. Previously in the RAFT dispersion polymerization of MEA, we found that such higher-molecular-weight shoulders could be minimized by using a low ratio (0.02, relative to macro-CTA) of a redox initiator couple and a low polymerization temperature (30 °C).[59] However, in the current dispersion copolymerization system where the thermosensitive copolymers need to collapse to form particles, a relatively high temperature (70 °C) is necessary for the successful formation of nanogels, which can lead to a higher degree of transfer to polymer. Indeed, analysis of $\ln(M_0/M)$ *vs.* time indicated reduced polymerization rate at high monomer conversion (Fig. S4†), though dispersion polymerization is more complex than solution polymerization. Through optimization of polymerization, 0.05 equivalent V-50 seemed to be optimal in terms that a reasonably fast polymerization rate and a relatively small shoulder on the chromatograms could be obtained.

Having established that the aqueous dispersion copolymerization of MEA with PEGA was under good RAFT control, we further studied the production of nanogels *via* dispersion copolymerization in the presence of PEGDA cross-linker (Scheme 2). For these experiments, the molar ratio of PDMA : PEGDA was controlled to be 1 : 3, while the molar ratio of MEA/PEGA, the DP, the monomer content and thus the final solids content were systematically varied in order to produce nanogels with adjustable size at highest possible solid content (Table 2). The composition of the nanogels was analyzed by ^{1}H NMR (Fig. S2†). The diameter of the nanogels synthesized under such conditions ranges from 30 to 100 nm as determined by dynamic light scattering (DLS), and atomic force microscopy (AFM) image (Fig. 7A) confirms that spherical nanoparticles are formed and reflects the polydispersity determined by DLS. Transmission electron microscopy (TEM) (Fig. S5†) was also performed, though imaging of such soft nanogels is typically a challenging task. Most of the nanogels exhibit reduction in diameter upon temperature change from 20 °C to 60 °C except one case (entry 4, Table 2), which is due to the relatively low DP (80) of the thermosensitive block. Most of the nanogels show excellent colloidal stability except two examples (entries 3 and 11, Table 2) that display bimodal size distribution at 60 °C. At monomer loading of 10% but increasing the DP from 100 (entries 1–3, Table 2), 120 (entry 5, Table 2), 150 (entry 6, Table 2), to 200 (entries 7–9, Table 2), defined nanogels are produced except the case for entry 7 in Table 2, which actually forms a gel. When maintaining DP = 100 and molar ratio of MEA : PEGA = 85 : 15 but increasing the monomer loading from 10% to 30% (entries 2 and 10–12, Table 2), a gel is obtained at 30% while in all the other cases nanogels are produced. Similarly, when maintaining DP = 200 and molar ratio of MEA : PEGA = 85 : 15 but increasing the monomer loading from 10% to 25% (entries 8 and 13–15, Table 2), nanogels are only produced at 10% and 15% with a semi-gel and a gel produced at 20% and 25%, respectively. Through optimization of

Table 2 Synthetic conditions and results of nanogels produced by RAFT dispersion copolymerization of MEA with PEGA in the presence of PEGDA.[a]

	Macro-CTA	MEA	PEGA	PEGDA	Monomer (%)[b]	Solid (%)[c]	Conv. (%)[d]	D_h (nm), PDI at 20 °C[e]	D_h (nm), PDI at 60 °C[e]
1	1	90	10	3	10	12.5	98	42, 0.05	36, 0.09
2	1	85	15	3	10	12.3	98	33, 0.13	29, 0.24
3	1	80	20	3	10	12.1	96	37, 0.17	15 (92.8%), 5560 (7.2%)[f]
4	1	68	12	3	10	12.9	97	28, 0.17	31, 0.27
5	1	102	18	3	10	11.8	98	39, 0.11	30, 0.18
6	1	127.5	22.5	3	10	11.4	97	45, 0.12	34, 0.08
7	1	180	20	3	10	11.0	gel	—	—
8	1	170	30	3	10	10.9	91	35, 0.21[g]	—
9	1	160	40	3	10	10.8	95	57, 0.23[g]	—
10	1	85	15	3	20	24.5	100	37, 0.10	31, 0.08
11	1	85	15	3	25	30.6	100	46, 0.20	29 (97.6%), 5560 (2.4%)[f]
12	1	85	15	3	30	36.8	gel	—	—
13	1	170	30	3	15	16.7	100	99, 0.18	83, 0.19
14	1	170	30	3	20	22.3	semi-gel	—	—
15	1	170	30	3	25	27.9	gel	—	—

[a] 0.05 equivalent V-50, 70 °C, 5 h. The feed of macro-CTA, MEA, PEGA, and PEGDA are listed in molar ratios. [b] Monomer (MEA + PEGA + PEGDA) weight/water volume. [c] Solid weight/water volume. [d] Monomer conversion determined by ^{1}H NMR. [e] Hydrodynamic diameter and PDI determined by dynamic light scattering (DLS) at different temperatures. [f] Bimodal distribution of particle size with peak values listed. [g] Determined by DLS at 25 °C.

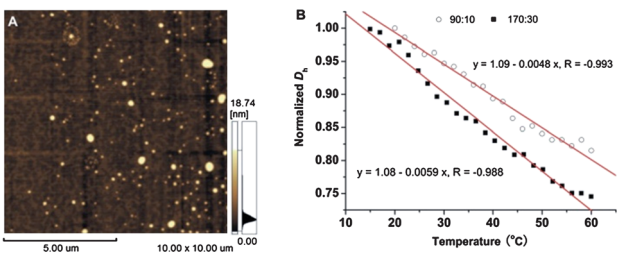

Fig. 7 (A) AFM micrograph of nanogel (entry 3, Table 2); (B) dependence of normalized D_h on temperature for nanogels synthesized with the molar ratio of MEA:PEGA being 90 : 10 and 170 : 30.

experimental conditions, thermosensitive nanogels with excellent stability can be produced at 20% monomer loading and 24.5% total solid content, which are reasonably high values for aqueous dispersion polymerization systems and represent an order of magnitude improvement in comparison with nanogel synthesis using MEO_2MA-based polymers.

From Table 2 we can see that most of the nanogels display a temperature-induced diameter reduction when raising the temperature from 20 °C to 60 °C. Fig. 7B illustrates the size dependence on temperature for two selected nanogel samples with MEA/PEGA ratios of 90 : 10 and 170 : 30, respectively. In stark contrast to the sharp thermal transitions of the corresponding copolymers of P(MEA-*co*-PEGA), these nanogels display a rather continuous diameter change upon raising temperature. For the microgels of MEO_2MA-based polymers prepared by traditional radical polymerization, Hu and co-workers[50] found that the phase transition of the microgels were broader than the LCST transition of the corresponding copolymers synthesized by ATRP,[25] and they concluded that the broadening in microgel phase transition was due to the broadening in the molecular weight distribution in traditional free radical process. Indeed, several studies have indicated that the LCST of thermosensitive polymers is dependent on the molecular weight of narrow dispersity polymers synthesized by controlled radical polymerization.[26,75,76] In microgels of MEO_2MA-based polymers synthesized by ATRP miniemulsion, although the phase transition is still broader than the LCST transition of the corresponding copolymers, defined phase transitions well correlated to the LCST of the same copolymer composition can be identified. Our RAFT dispersion copolymerization of MEA and PEGA has been demonstrated to have fairly good control over the molecular weight distribution with M_w/M_n smaller than 1.15. Therefore, the continuous reduction in size of these nanogels cannot be explained by broadening in molecular weight distribution. We further performed linear analysis for the thermal profiles of the nanogels and found that a reasonably good linear relationship can be obtained for both nanogels over a temperature range of 20–60 °C. Recently, Jiang and co-workers reported a linear relationship of the temperature-dependent photoluminescence of Eu(III) phthalate coordinated to the PNIPAM shell of polystyrene-*co*-PNIPA (core)—PNIPAM (shell) nanoparticles over the temperature range of 10–50 °C, which is different to the discontinuous thermal transition of the corresponding nanoparticles without Eu(III) phthalate.[77] However, to the best of our knowledge, linear dependence of thermal transition of nanogels/microgels alone has not been reported. At the current stage, the exact mechanism of the linear response of our nanogels is not clear. The unexpected linear response of the nanogels is, however, very interesting in that it compensates the discontinuous thermal transitions of most of the nanogels currently studied and may find application in areas that require linear transitions with temperature.

Conclusions

We have developed thermosensitive copolymers of P(MEA-*co*-PEGA) that have tunable LCST. Using MEA as the majority comonomer, the solid content of RAFT dispersion copolymerization system has been significantly improved to 24.5%, compared to the only several percents in the nanogel synthesis using MEO_2MA as the majority monomer. The dispersion copolymerization of MEA with PEGA showed excellent RAFT

control up to 100% monomer conversion using PDMA as both the RAFT agent and the stabilizer. The synthesized nanogels are in the range of 30–100 nm and exhibited good stability. The diameter of the nanogels exhibits an unexpected linear dependence on temperature over a broad range.

Experimental

Materials

2-Methoxyethyl acrylate (MEA, 98%), poly(ethylene glycol) methyl ether acrylate (PEGA, M_n = 480), poly(ethylene glycol) diacrylate (PEGDA, M_n = 258), and 2,2′-azobis(2-methylpropionamidine) dihydrochloride (V-50, 97%) were purchased from Sigma-Aldrich. *N*,*N*′-Dimethylacrylamide (98%) was purchased from J&K. *N*,*N*′-Dimethylformamide (DMF, 99.5+%), tetrahydrofuran (THF, 99+%), diethyl ether anhydrous (99.7+%), 2,2′-azobis(2-methylpropionitrile) (AIBN, CP) were purchased from Sinopharm Chemical Reagent Co. Ltd. AIBN was recrystallized from methanol twice. All monomers were passed through a column of Al_2O_3 to remove the inhibitor before use.

Characterization

NMR spectra were collected on a Bruker AV 500 MHz spectrometer and chemical shifts were reported using the solvent residue as the reference. Gel permeation chromatography (GPC) was performed on a Waters Alliance e2695 GPC system, equipped with a styragel guard column, a Waters styragel HR3 (molecular weight range 5.0×10^2–3.0×10^4), a Waters styragel HR4 (molecular weight range 5.0×10^3–6.0×10^5), and a Waters styragel HR5 (molecular weight range 5.0×10^4–4.0×10^6). Detection was performed on a 2414 refractometer using DMF (HPLC grade, containing 0.1 mg mL^{-1} LiBr) as the eluent at a flow rate of 0.8 mL min^{-1}. The temperature of the columns was set at 65 °C and the temperature of the refractometer was set at 45 °C. Analysis of molecular weight and polydispersity index of polymers was performed using Empower 2 software against PMMA standard (molecular weight range 2.4×10^2–1.0×10^6). LCST measurements were conducted by turbidimetry on a Hitachi U-3010 UV-vis spectrometer, and the temperature was varied at one degree internals. Nanoparticle sizing was analyzed using dynamic light scattering (DLS) on a Malvern ZS90. Atomic force microscopy (AFM) was performed on a Shimadzu SPM-9600 in the tapping mode. Transmission electron microscopy (TEM) was performed on a JEOL 200CX electron microscope operating at 200 kV.

Synthesis of thermosenstitive copolymers

Thermosensitive copolymers, P(MEA-*co*-PEGA)s, were synthesized by RAFT copolymerization of MEA and PEGA of varied molar ratios in DMF at 70 °C. The concentration of chain transfer agent (CTA) was 29 mM, and the molar ratio of AIBN/CTA was 0.2. The target degree of polymerization (DP) was ~103–106, and the actual DP of all thermosensitive copolymers was around 100. An exemplary synthesis of the copolymers is given for P(MEA_{86}-*co*-$PEGA_{10}$). CTA benzyl ethyl trithiocarbonate[78] (66.4 mg, 0.29 mmol), MEA (3.60 g, 27.70 mmol), PEGA (1.47 g, 3.10 mmol), and 1,3,5-trioxane (0.28 g, 3.08 mmol, internal standard) were dissolved in 10 mL of DMF. The solution was degassed with nitrogen at 0 °C for 40 min before immersion into a preheated oil bath at 70 °C. After the temperature was stabilized, a degassed solution of AIBN (10.1 mg, 0.062 mmol) in DMF was injected *via* a microsyringe. Aliquots were sampled at predetermined time intervals for polymerization kinetics study. The conversion of monomers was calculated to be 92% for 3 h polymerization by comparing the vinyl signals of the monomers at 6.40, 6.18 and 5.98 ppm with the signal of 1,3,5-trioxane at 5.16 ppm. M_n = 15 000 (NMR), M_n = 30 000 (GPC), M_w/M_n = 1.15 (GPC).

Synthesis of poly(*N*,*N*′-dimethylacrylamide) (PDMA) macro-CTA

Benzyl ethyl trithiocarbonate (1.008 g, 4.41 mmol), *N*,*N*′-dimethylacrylamide (35.0 g, 0.35 mol), and 1,3,5-trioxane (7.0 g, 77.78 mmol, internal standard) were dissolved in DMF (70 mL). The solution was degassed with nitrogen at 0 °C for 30 min before immersion into a preheated oil bath at 70 °C. After the temperature was stabilized, a degassed AIBN DMF solution (20 μL, 14.5 mg, 0.088 mmol) was injected *via* a microsyringe. The polymerization was conducted for 4 h and was stopped at 61% monomer conversion as determined by ^{1}H NMR. The polymerization was quenched by immersing the polymerization flask into an ice/water bath and exposing to air. The solution was diluted and the polymer was precipitated into ethyl ether. The polymer was collected by centrifugation and purified one more time by precipitation of the polymer THF solution into ethyl ether. After drying under vacuum, 19.0 g of a yellow solid was obtained in 53% yield. M_n = 5000 (^{1}H NMR), M_n = 8000 (GPC), M_w/M_n = 1.10.

RAFT dispersion polymerization

RAFT dispersion polymerization of MEA and PEGA of varied molar ratios was carried out in water at 70 °C using PDMA macro-CTA either in the absence or in the presence of the cross-linker PEGDA for block copolymer or nanogel synthesis, respectively. The molar ratios of V-50/macro-CTA and PEGDA/macro-CTA were controlled at 0.05 : 1 and 3 : 1, respectively. The target DPs were 80, 100, 120, 150, and 200. A typical dispersion polymerization with a target DP of 85 for MEA and a target DP of 15 for PEGA is as follows. Macro-CTA (0.106 g, 0.021 mmol), MEA (0.232 g, 1.79 mmol), and PEGA (0.151 g, 0.32 mmol) were dissolved in 4 mL of water. The solution was degassed with nitrogen at 0 °C for at least 40 min before immersion into a preheated oil bath at 70 °C. After the temperature was stabilized, a degassed solution of V-50 (0.3 mg, 1.1 μmol) was injected *via* a microsyringe. The polymerization was allowed to continue under protection of nitrogen. Aliquots were withdrawn at predetermined time intervals and were quenched in iced water. The conversion of monomers was calculated by comparing the vinyl signals of the monomers at 6.35, 6.10 and 5.88 ppm with the ester methylene group signals at 4.23 ppm.

Acknowledgements

This work is supported by National Basic Research Program of China (2009CB930200), National Natural Science Foundation

of China (20904029), Shanghai Pujiang Program (09PJ1404800), Program for Professor of Special Appointment (Eastern Scholar) at Shanghai Institutions of Higher Learning, Foundation for Excellent Youth Scholar of Higher Education of Shanghai, and Shanghai Leading Academic Disciplines (S30109). We thank Dr Hongmei Deng at Instrumental Analysis and Research Center, Shanghai University for assistance with NMR.

Notes and references

1 M. A. C. Stuart, W. T. S. Huck, J. Genzer, M. Muller, C. Ober, M. Stamm, G. B. Sukhorukov, I. Szleifer, V. V. Tsukruk, M. Urban, F. Winnik, S. Zauscher, I. Luzinov and S. Minko, *Nat. Mater.*, 2010, **9**, 101–113.
2 R. J. Wojtecki, M. A. Meador and S. J. Rowan, *Nat. Mater.*, 2011, **10**, 14–27.
3 M. A. Hempenius, C. Cirmi, F. Lo Savio, J. Song and G. J. Vancso, *Macromol. Rapid Commun.*, 2010, **31**, 772–783.
4 P. Brochu and Q. Pei, *Macromol. Rapid Commun.*, 2010, **31**, 10–36.
5 C. Ohm, M. Brehmer and R. Zentel, *Adv. Mater.*, 2010, **22**, 3366–3387.
6 M. Behl, M. Y. Razzaq and A. Lendlein, *Adv. Mater.*, 2010, **22**, 3388–3410.
7 C. Liu, H. Qin and P. T. Mather, *J. Mater. Chem.*, 2007, **17**, 1543–1558.
8 A. Brun-Graeppi, C. Richard, M. Bessodes, D. Scherman and O. W. Merten, *Prog. Polym. Sci.*, 2010, **35**, 1311–1324.
9 G. Pasparakis and M. Vamvakaki, *Polym. Chem.*, 2011, **2**, 1234–1248.
10 J. L. Zhang and Y. C. Han, *Chem. Soc. Rev.*, 2010, **39**, 676–693.
11 H. Nandivada, A. M. Ross and J. Lahann, *Prog. Polym. Sci.*, 2010, **35**, 141–154.
12 N. M. Alves, I. Pashkuleva, R. L. Reis and J. F. Mano, *Small*, 2010, **6**, 2208–2220.
13 L. S. Zha, B. Banik and F. Alexis, *Soft Matter*, 2011, **7**, 5908–5916.
14 S. R. MacEwan, D. J. Callahan and A. Chilkoti, *Nanomedicine*, 2010, **5**, 793–806.
15 I. K. Park, K. Singha, R. B. Arote, Y. J. Choi, W. J. Kim and C. S. Cho, *Macromol. Rapid Commun.*, 2010, **31**, 1122–1133.
16 D. D. Diaz, D. Kuhbeck and R. J. Koopmans, *Chem. Soc. Rev.*, 2011, **40**, 427–448.
17 J. A. Wang, J. Mei, A. J. Qin, J. Z. Sun and B. Z. Tang, *Sci. China Chem.*, 2010, **53**, 2409–2428.
18 A. Pucci, R. Bizzarri and G. Ruggeri, *Soft Matter*, 2011, **7**, 3689–3700.
19 F. Ercole, T. P. Davis and R. A. Evans, *Polym. Chem.*, 2010, **1**, 37–54.
20 I. Dimitrov, B. Trzebicka, A. H. E. Muller, A. Dworak and C. B. Tsvetanov, *Prog. Polym. Sci.*, 2007, **32**, 1275–1343.
21 Z. M. O. Rzaev, S. Dincer and E. Piskin, *Prog. Polym. Sci.*, 2007, **32**, 534–595.
22 W. Li, A. Zhang, K. Feldman, P. Walde and A. D. Schluter, *Macromolecules*, 2008, **41**, 3659–3667.
23 T. Gillich, E. M. Benetti, E. Rakhmatullina, R. Konradi, W. Li, A. Zhang, A. D. Schluter and M. Textor, *J. Am. Chem. Soc.*, 2011, **133**, 10940–10950.
24 R. Hoogenboom, H. M. L. Thijs, M. J. H. C. Jochems, B. M. van Lankvelt, M. W. M. Fijten and U. S. Schubert, *Chem. Commun.*, 2008, 5758–5760.
25 J.-F. Lutz and A. Hoth, *Macromolecules*, 2006, **39**, 893–896.
26 J.-F. Lutz, O. Akdemir and A. Hoth, *J. Am. Chem. Soc.*, 2006, **128**, 13046–13047.
27 J.-F. Lutz, *J. Polym. Sci., Part A: Polym. Chem.*, 2008, **46**, 3459–3470.
28 J.-F. Lutz, *Adv. Mater.*, 2011, **23**, 2237–2243.
29 K. Yang, X. Wei, F. Wu, C. Cao, J. Deng and Y. Cai, *Soft Matter*, 2011, **7**, 5861–5872.
30 R. Paris and I. Quijada-Garrido, *Eur. Polym. J.*, 2009, **45**, 3418–3425.
31 Z. Zarafshani, T. Obata and J.-F. Lutz, *Biomacromolecules*, 2010, **11**, 2130–2135.
32 G. Sun and Z. Guan, *Macromolecules*, 2010, **43**, 9668–9673.
33 Z.-Y. Qiao, F.-S. Du, R. Zhang, D.-H. Liang and Z.-C. Li, *Macromolecules*, 2010, **43**, 6485–6494.
34 S. Park, H. Y. Cho, J. A. Yoon, Y. Kwak, A. Srinivasan, J. O. Hollinger, H.-j. Paik and K. Matyjaszewski, *Biomacromolecules*, 2010, **11**, 2647–2652.
35 T. G. O'Lenick, X. Jiang and B. Zhao, *Langmuir*, 2010, **26**, 8787–8796.
36 K. T. Wiss, O. D. Krishna, P. J. Roth, K. L. Kiick and P. Theato, *Macromolecules*, 2009, **42**, 3860–3863.
37 M. W. Jones, M. I. Gibson, G. Mantovani and D. M. Haddleton, *Polym. Chem.*, 2011, **2**, 572–574.
38 R. París and I. Quijada-Garrido, *Eur. Polym. J.*, 2009, **45**, 3418–3425.
39 G. Pasparakis and C. Alexander, *Angew. Chem., Int. Ed.*, 2008, **47**, 4847–4850.
40 Z. Ge, Y. Zhou, J. Xu, H. Liu, D. Chen and S. Liu, *J. Am. Chem. Soc.*, 2009, **131**, 1628–1629.
41 W. Wang, H. Liang, R. Cheikh Al Ghanami, L. Hamilton, M. Fraylich, K. M. Shakesheff, B. Saunders and C. Alexander, *Adv. Mater.*, 2009, **21**, 1809–1813.
42 M. I. Gibson, D. Paripovic and H.-A. Klok, *Adv. Mater.*, 2010, **22**, 4721–4725.
43 A. M. Jonas, K. Glinel, R. Oren, B. Nysten and W. T. S. Huck, *Macromolecules*, 2007, **40**, 4403–4405.
44 X. Laloyaux, E. Fautré, T. Blin, V. Purohit, J. Leprince, T. Jouenne, A. M. Jonas and K. Glinel, *Adv. Mater.*, 2010, **22**, 5024–5028.
45 C. Boyer, M. R. Whittaker, M. Luzon and T. P. Davis, *Macromolecules*, 2009, **42**, 6917–6926.
46 E. Wischerhoff, K. Uhlig, A. Lankenau, H. G. Borner, A. Laschewsky, C. Duschl and J. F. Lutz, *Angew. Chem., Int. Ed.*, 2008, **47**, 5666–5668.
47 M. Luzon, C. Boyer, C. Peinado, T. Corrales, M. Whittaker, L. Tao and T. P. Davis, *J. Polym. Sci., Part A: Polym. Chem.*, 2010, **48**, 2783–2792.
48 Z. An, Q. Qiu and G. Liu, *Chem. Commun.*, 2011, **47**, 12424–12440.
49 Z. B. Hu, T. Cai and C. L. Chi, *Soft Matter*, 2010, **6**, 2115–2123.
50 T. Cai, M. Marquez and Z. B. Hu, *Langmuir*, 2007, **23**, 8663–8666.
51 T. Cai, G. N. Wang, S. Thompson, M. Marquez and Z. B. Hu, *Macromolecules*, 2008, **41**, 9508–9512.
52 C. L. Chi, T. Cai and Z. B. Hu, *Langmuir*, 2009, **25**, 3814–3819.
53 T. Zhou, W. Wu and S. Zhou, *Polymer*, 2010, **51**, 3926–3933.
54 H. C. Dong and K. Matyjaszewski, *Macromolecules*, 2010, **43**, 4623–4628.
55 H. C. Dong, V. Mantha and K. Matyjaszewski, *Chem. Mater.*, 2009, **21**, 3965–3972.
56 Z. An, Q. Shi, W. Tang, C.-K. Tsung, C. J. Hawker and G. D. Stucky, *J. Am. Chem. Soc.*, 2007, **129**, 14493–14499.
57 Z. An, W. Tang, M. Wu, Z. Jiao and G. D. Stucky, *Chem. Commun.*, 2008, 6501–6503.
58 W. Shen, Y. Chang, G. Liu, H. Wang, A. Cao and Z. An, *Macromolecules*, 2011, **44**, 2524–2530.
59 G. Liu, Q. Qiu, W. Shen and Z. An, *Macromolecules*, 2011, **44**, 5237–5245.
60 M. Tanaka, A. Mochizuki, N. Ishii, T. Motomura and T. Hatakeyama, *Biomacromolecules*, 2002, **3**, 36–41.
61 M. Tanaka, T. Motomura, M. Kawada, T. Anzai, Y. Kasori, T. Shiroya, K. Shimura, M. Onishi and A. Mochizuki, *Biomaterials*, 2000, **21**, 1471–1481.
62 K. Skrabania, J. Kristen, A. Laschewsky, O. Akdemir, A. Hoth and J. F. Lutz, *Langmuir*, 2007, **23**, 84–93.
63 W. Steinhauer, R. Hoogenboom, H. Keul and M. Moeller, *Macromolecules*, 2010, **43**, 7041–7047.
64 C. Lavigueur, J. G. García, L. Hendriks, R. Hoogenboom, J. J. L. M. Cornelissen and R. J. M. Nolte, *Polym. Chem.*, 2011, **2**, 333–340.
65 M. J. Zhong and K. Matyjaszewski, *Macromolecules*, 2011, **44**, 2668–2677.
66 Y. Reyes and J. M. Asua, *Macromol. Rapid Commun.*, 2011, **32**, 63–67.
67 N. M. Ahmad, B. Charleux, C. Farcet, C. J. Ferguson, S. G. Gaynor, B. S. Hawkett, F. Heatley, B. Klumperman, D. Konkolewicz, P. A. Lovell, K. Matyjaszewski and R. Venkatesh, *Macromol. Rapid Commun.*, 2009, **30**, 2002–2021.
68 F. J. Lu, Y. W. Luo, B. G. Li, Q. Zhao and F. J. Schork, *Macromolecules*, 2010, **43**, 568–571.
69 Y. Wang, G. H. Jiang, M. Zhang, L. Wang, R. J. Wang and X. K. Sun, *Soft Matter*, 2011, **7**, 5348–5352.

70 J. Rieger, C. Grazon, B. Charleux, D. Alaimo and C. Jerome, *J. Polym. Sci., Part A: Polym. Chem.*, 2009, **47**, 2373–2390.
71 L. F. Yan and W. Tao, *Polymer*, 2010, **51**, 2161–2167.
72 C. Grazon, J. Rieger, N. Sanson and B. Charleux, *Soft Matter*, 2011, **7**, 3482–3490.
73 Q. Qiu, G. Liu and Z. An, *Chem. Commun.*, 2011, **47**, 12685–12687.
74 J. Rieger, W. J. Zhang, F. Stoffelbach and B. Charleux, *Macromolecules*, 2010, **43**, 6302–6310.
75 Y. Xia, X. Yin, N. A. D. Burke and H. D. H. Stöver, *Macromolecules*, 2005, **38**, 5937–5943.
76 S. Furyk, Y. J. Zhang, D. Ortiz-Acosta, P. S. Cremer and D. E. Bergbreiter, *J. Polym. Sci., Part A: Polym. Chem.*, 2006, **44**, 1492–1501.
77 Y. Jiang, X. Yang, C. Ma, C. Wang, H. Li, F. Dong, X. Zhai, K. Yu, Q. Lin and B. Yang, *Small*, 2010, **6**, 2673–2677.
78 W. Shen, Q. Qiu, Y. Wang, M. Miao, B. Li, T. Zhang, A. Cao and Z. An, *Macromol. Rapid Commun.*, 2010, **31**, 1444–1448.

